Application of the thermography method for determining the fatigue limit of a nickel alloy produced by wire-arc additive manufacturing

Michael Nikhamkin, Dmitriy Trushnikov, Sergey Neulybin, Danil Solomonov, Ivan Konev
Perm National Research Polytechnic University, Russia
nikhamkin@mail.ru, http://orcid.org/0000-0002-3649-4482
trdimitr@yandex.ru, http://orcid.org/0000-0001-7105-7934
sergeyneulybin@gmail.com, http://orcid.org/0000-0003-1846-1502
solomonov1198@yandex.ru, http://orcid.org/0000-0003-2577-3037
konev@perm.ru, http://orcid.org/0000-0002-8192-1682

Citation: Nikhamkin, M., Trushnikov, D., Neulybin, S., Solomonov, D., Konev, I., Application of the thermography method for determining the fatigue limit of a nickel alloy produced by wire-arc additive manufacturing, Fracture and Structural Integrity, 75 (2026) 390-398.

Received: 08.10.2025
Accepted: 02.12.2025
Published: 08.12.2025
Issue: 01.2026

KEYWORDS. Additive manufacturing, Wire-are deposition, Heat-resistant nickel alloy, High-cycle fatigue, Fatigue limit, Infrared thermography method.

INTRODUCTION

Additive manufacturing (AM) of metal parts is gaining increasing significance across various industries owing to fundamentally new technological capabilities unattainable with conventional methods. Additive technologies have been successfully applied in aerospace, construction, biomedicine and other sectors. In recent years, there has been rapid development of processes for producing billets from heat-resistant nickel alloys by wire-arc additive manufacturing (WAAM) with subsequent machining. Characteristic features of this method are the ability to obtain large billets with minimal allowance and high mechanical properties, as well as the relative affordability of the equipment [1-4].

The development of additive technologies for manufacturing safety-critical components must be accompanied by a thorough analysis of the material's resistance to high-cycle fatigue (HCF). Fatigue resistance is particularly sensitive to micro-defects that can arise during AM. As shown in a recent review [5], the HCF properties of additively manufactured metals are generally lower than those of their conventionally produced counterparts with comparable static strength. The most important factors determining the fatigue properties of AM metals are microstructure, anisotropy and defects induced by technological factors. To improve HCF performance, heat treatment and surface strengthening are applied [5, 6].

A study [7] of the high-cycle fatigue of Inconel 625 produced by Selective Laser Melting used the "short staircase" method to determine the fatigue limit. The authors noted that the formation of process-induced defects is one of the main issues significantly affecting fatigue properties. A similar conclusion was drawn in another study on the high-cycle fatigue of Inconel 625 [8].

In recent years, more and more researchers have been using the Thermographic Method (Risitano method) or the IRT method (Infra-Red Thermography) for this purpose. This method was developed in the 1990s in [9, 10], initially to assess the fatigue limit. The authors of [11] proposed expanding this method to obtain a fatigue curve.

The Thermographic Method is based on the self-heating effect of a material under cyclic loading due to energy dissipation associated with the accumulation of fatigue damage. The specimen is subjected to a sequence of cyclic loading blocks with increasing load. When the amplitude of alternating stresses exceeds the fatigue limit, the process of fatigue damage accumulation is initiated, which is manifested by the activation of self-heating and an increase in the specimen temperature. Currently, various versions of the Thermographic Method for assessing the characteristics of high-cycle fatigue resistance have been developed, widely presented in the literature and described in detail in recent reviews [12, 13]. Numerous studies have shown that fatigue limit estimates based on temperature changes in metallic materials are close to those obtained by traditional methods (see, for example, [14, 15]). In [16], it was shown that this method can be used to assess the accumulation of fatigue damage and evaluate fatigue life under variable stress amplitude. Yang et al. [17] proposed an approach using a Thermographic Method to obtain three-parameter P–S–N fatigue curves for metals.

In [18], several Thermographic Method variants are compared: the classical Risitano method, a method based on measuring the sample temperature under static loading, and methods based on the "second harmonic". It is shown that for the steels studied, these methods provide a very good engineering estimate of the fatigue limit compared to "ladder" testing.

In [19], infrared thermography was used to study the characteristic patterns of energy dissipation during fatigue failure of nanostructured titanium. In [20], a study was conducted on the fatigue behavior of 316L stainless steel specimens manufactured using Selective Laser Melting. The results confirm the effectiveness of the Thermographic Method for assessing the fatigue limit of such materials. Zhang H. et al. [21] used the Thermographic Method to accelerate the assessment of the fatigue limit when selecting options for Selective Laser Melting technology for 304L steel. A similar problem was solved using this method by Douellou C. et al. [22] in relation to the selection of process parameters for laser cladding in a powder bed of martensitic steel.

The conducted analysis of the state of research on the application of the Thermographic Method to determine the characteristics of high-cycle fatigue resistance of metals, the practical use of this method for new materials requires clarification of test methods in terms of the selection of specimen parameters, equipment, detection parameters, the choice of parameters characterizing energy dissipation, and the methods for processing the results. The aim of this work is to develop, within the framework of the infrared thermography method, and validate an accelerated technique for assessing the fatigue limit of nickel alloy samples manufactured using additive wire surfacing technology.

MATERIALS AND METHODS

The object of study is Inconel 625 produced by additive manufacturing using wire-arc deposition. The material was fabricated at the Laboratory of Methods for Creating and Designing "material–technology–structure" Systems of Perm National Research Polytechnic University.

The 3D-printing process uses specialised equipment. The equipment layout is shown in Fig. 1. The equipment must ensure the tool path for deposition in accordance with the 3D model of the part. This path is implemented through a control program—a slicer—which converts the 3D model into a set of flat two-dimensional layers that form the billet configuration layer by layer. 3D printing is performed on a substrate sheet 10 mm thick. As filler material, wire made of Inconel 625 with a diameter of 1.2 mm (tolerance –0.12 mm) is used.

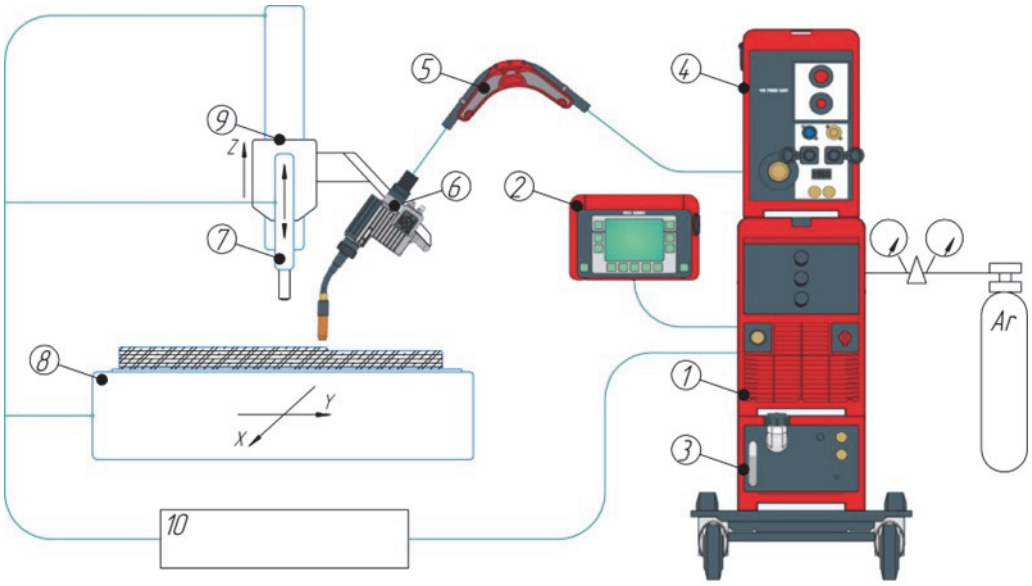

Figure 1: Technological process diagram. (1 – welding power source, 2 – control panel, 3 – chiller, 4 – wire feed unit, 5 – wire buffer, 6 – welding torch, 7 – pneumatic hammer, 8 – substrate, 9 – pneumatic-tool holder, 10 – CNC control system).

Deposition is carried out using short-circuit transfer with the following parameters: arc current I=140-170 A, arc voltage U=13-15 V, wire feed speed V=6.0-7.0 m/min, torch travel speed V_{dep} =40-50 cm/min, and argon shielding gas flow rate Q=25 L/min. The deposited layers are plastically deformed by a pneumatic hammer with: hammer travel speed V=300 mm/min, hammer frequency N=2820 impacts/min, impact energy E=19.74 J, hemispherical striker radius R=30 mm, and pressing force 300 N. The layers are forged at T=200-300 °C. After 3D printing, the walls are heat-treated [2].
For fatigue tests, flat specimens 1.5 mm thick were cut from the WAAM billet using electro-erosion (see Fig. 2). The specimen surfaces were ground along the specimen's long axis.

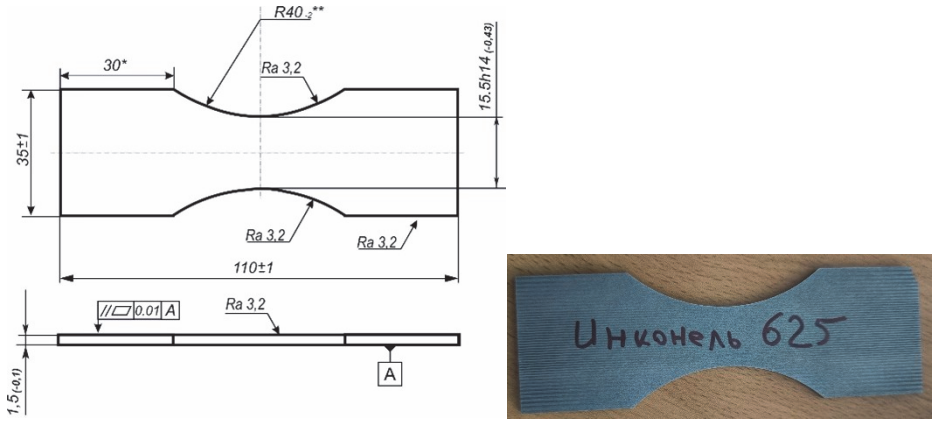

Figure 2: Samples for high-cycle fatigue testing: drawing (left) and appearance (right).

For the correct use of thermographic analysis, it is critical that the temperature be uniform across the sample thickness. The Biot criterion (see, for example, Zhao A. [23]) can be used to assess the acceptability of this assumption. According to this criterion, the temperature gradient across the thickness of the samples being studied is negligible.
High-cycle fatigue tests were conducted under uniaxial cyclic tension using a high-frequency resonant testing machine Testronic-50 (Fig. 3) at the Laboratory for High-Cycle Fatigue Research of Perm National Research Polytechnic University. Testing employed a "soft" loading cycle with constant mean and amplitude stresses. The asymmetry ratio was $R=\sigma_{min}/\sigma_{max}=0.1$. The loading frequency was 125 Hz, and tests were performed at room temperature.
For accelerated fatigue-limit determination, an experimental technique oriented towards additive nickel superalloys was developed within the IRT framework. According to this method, specimen loading consists of a sequence of blocks with

constant cyclic loading parameters: minimum σ_{min} and maximum σ_{max} stresses in the cycle (Fig. 4). In each successive block the maximum stress increases by a step $\Delta\sigma_{max}$. After each block the specimen is allowed to cool to its initial temperature. During loading, the temperature field on the specimen surface is recorded by an infrared camera. In the present work an NEC TH9100 WR ProNew camera operating in the 8–14 μm range with sensitivity 0.02 °C and a 320 × 240 pixel detector was used. To reduce thermography errors, the room temperature is maintained constant during testing, and external infrared sources are screened. The specimen surface is coated with black matte paint before testing.

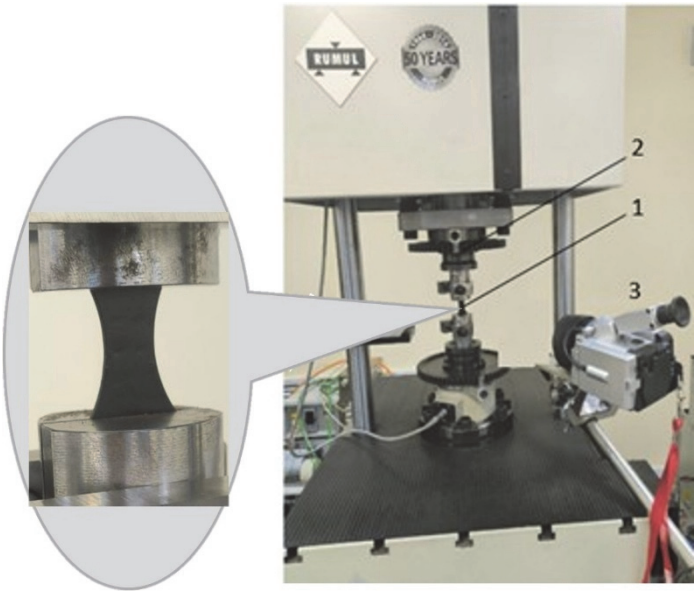

Figure 3: Experimental set-up. 1 – specimen, 2 – Testronic-50 testing machine, 3 – infrared camera.

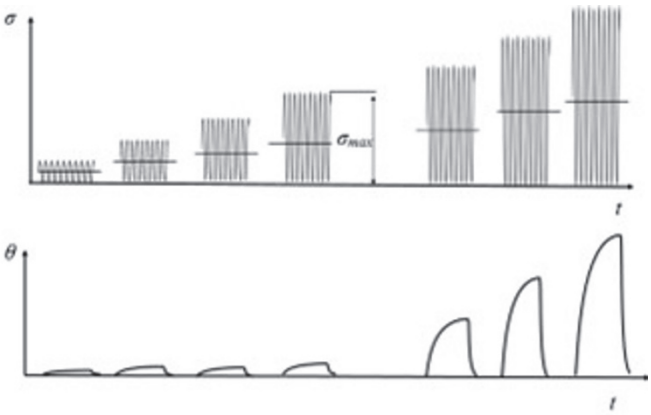

Figure 4: Block cyclic loading of a specimen (top) and typical temperature change on the specimen surface (bottom).

Developing a fatigue-limit determination method for a particular material involves, in addition to selecting equipment and specimen type, a justified choice of the number of loading blocks and their parameters—initial and final σ_{max} values and loading step $\Delta\sigma_{max}$. In addition, a region on the specimen surface for temperature recording must be specified, taking into account the non-uniform temperature field, and a heating indicator parameter must be selected in accordance with the IRT procedure.

Previous works [24] developed accelerated fatigue-limit assessment procedures for polymer composite materials within the IRT framework. They proposed processing elements to improve data accuracy.

Fig. 5 shows the temperature increment on the specimen surface $\theta=T-T_0$ (where T and T_0 are the current and initial temperatures) during cyclic loading with constant stress amplitude above the fatigue limit **Errore. L'origine riferimento non è stata trovata.**. Three stages of self-heating are distinguished: stage I – temperature increases due to energy dissipation associated with fatigue damage accumulation; stage II – temperature stabilises because all generated heat is dissipated to the

environment; stage III – just before failure, energy dissipation increases sharply, heat is not removed in time and the surface temperature rises again. During block loading, the block duration is usually limited to the onset of stage II.

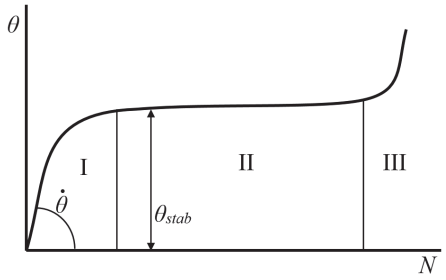

Figure 5: Typical dependence of temperature increment θ on the number of loading cycles N for σ_{max} above the fatigue limit [1].

As heating indicators, different authors [14, 15] use either the temperature increment on the surface at stabilization stage θ_{stab} or the rate of temperature increase at the beginning of the loading block θ̇ . It has been shown [24] that for materials with low thermal conductivity these parameters yield practically identical fatigue-limit values. Therefore, in this study the parameter θ̇ is used, whose determination requires fewer cycles per block.

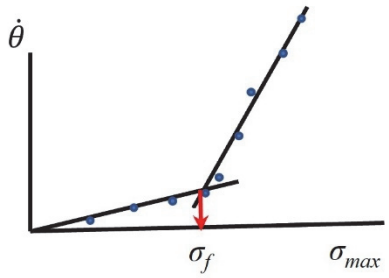

Figure 6: Determining the fatigue limit σ_f by infrared thermography.

To determine the fatigue limit in accordance with the IRT method, the dependence of the heating indicator on σ_{max} is used. This dependence can be divided into two branches: above and below the fatigue limit σ_f (Fig. 6). The value of σ_f is defined as the abscissa of the intersection point of the linear approximations of these branches. Separation of experimental points into two branches is not always obvious. To avoid subjectivity, several criteria have been proposed [14]. In this work, as in previous studies [13, 24], it is proposed to choose the branch separation point such that the sum of the coefficients of determination of the right and left branches R^2_1 and R^2_2 is maximized. The combined coefficient is:

$$R_{\Sigma}^2 = \frac{\left(R_1^2 + R_2^2\right)}{2} \tag{1}$$

RESULTS AND DISCUSSION

For fatigue-limit determination by IRT the loading consisted of 11 blocks. The maximum stress σ_{max} increased from block to block from 300 to 460 MPa with a step $\Delta\sigma_{max}$=10–20 MPa. The duration of each block 12 000 cycles was chosen to reliably record the rate of temperature rise at the block start.

Region A on the specimen surface, where the temperature field is recorded, is shown in Fig. 7. Given the non-uniform temperature field, both the average and maximum temperatures in this zone are used to determine the fatigue limit. Temperature non-uniformity along the specimen's length is associated with heat removal into the machine grips.

Fig. 8 shows the dependence of the maximum temperature increment in region A on the number of cycles. The displayed area corresponds to the start of loading blocks (stage I), where numerical differentiation yields the rate of temperature rise $\dot{\theta}_{max}$. An increase in θ̇ with increasing is evident.

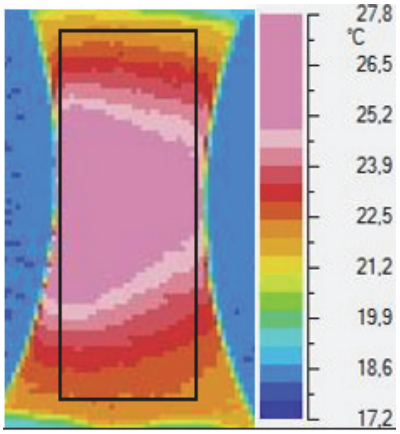

Figure 7: Example of a sample thermogram. The black rectangle is region A, in which the temperature field is recorded.

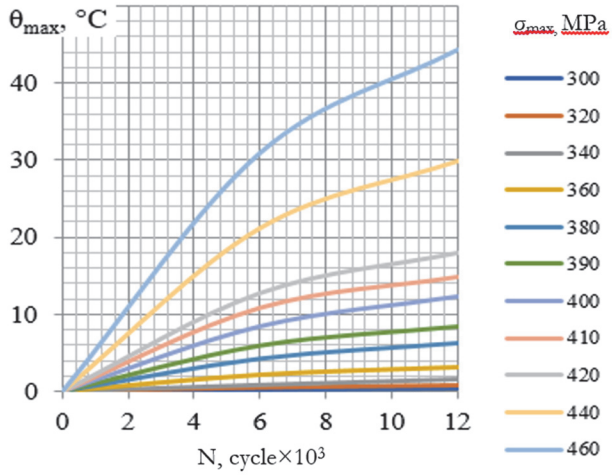

Figure 8: Dependence of the maximum temperature increase in region A on the number of loading cycles at different stress values σ_{max}.

To determine the fatigue limit, the rates of temperature rise at the beginning of loading blocks were calculated in four variants: maximum θ_{max} and average θ_{av} values in region A, each determined by differentiation over 6000 and 12 000 cycles. Fig. 9 shows the dependencies of these parameters on σ_{max}. Fatigue limits were determined as described above from the intersection point of bilinear approximations of the two branches of the heating indicator versus stress.

To formalize the selection of the branch separation point for the dependencies $\theta_{max}(\sigma_{max})$ and $\theta_{av}(\sigma_{max})$, the criterion of maximum combined coefficient of determination R^2_{Σ} (1) was used [16, 22]. Fig. 10 presents R^2_{Σ} values for different separation points k (k is the serial number of the loading block). The highest value corresponds to k=4.

Tab. 1 summarises the fatigue limits obtained by infrared thermography for the four heating indicators. All four variants give nearly identical fatigue limits; the mean value is 383 MPa, with a coefficient of variation of 0.46 %.

Heating indicator	Fatigue limit, MPa
θ_{av} (ΔN = 6000 cycles)	384.7
θ_{av} (ΔN = 12 000 cycles)	384.5
θ_{max} (ΔN = 6000 cycles)	381.3
θ_{max} (ΔN = 12 000 cycles)	381.9

Table 1: Fatigue-limit values obtained by infrared thermography.

Validation of the developed accelerated thermographic technique for determining the fatigue limit was performed using traditional fatigue tests with an S–N curve. Tests were conducted on a batch of Inconel 625 specimens produced by WAAM.

Specimens from the same batch as those used in the accelerated method were tested. The tests followed ASTM E466 requirements with the following deviations: specimen design as in Fig. 1; number of specimens – 10.

Tests were carried out on the Testronic-50 machine. As in the Thermographic Method, the specimens were tested under constant mean and amplitude stresses with asymmetry ratio R=0.1. The base number of cycles was $N_b=10^7$.

Results are presented in Fig. 11. The fatigue limit by the standard method for a 50 % probability of failure at 10^7 cycles is 399 MPa.

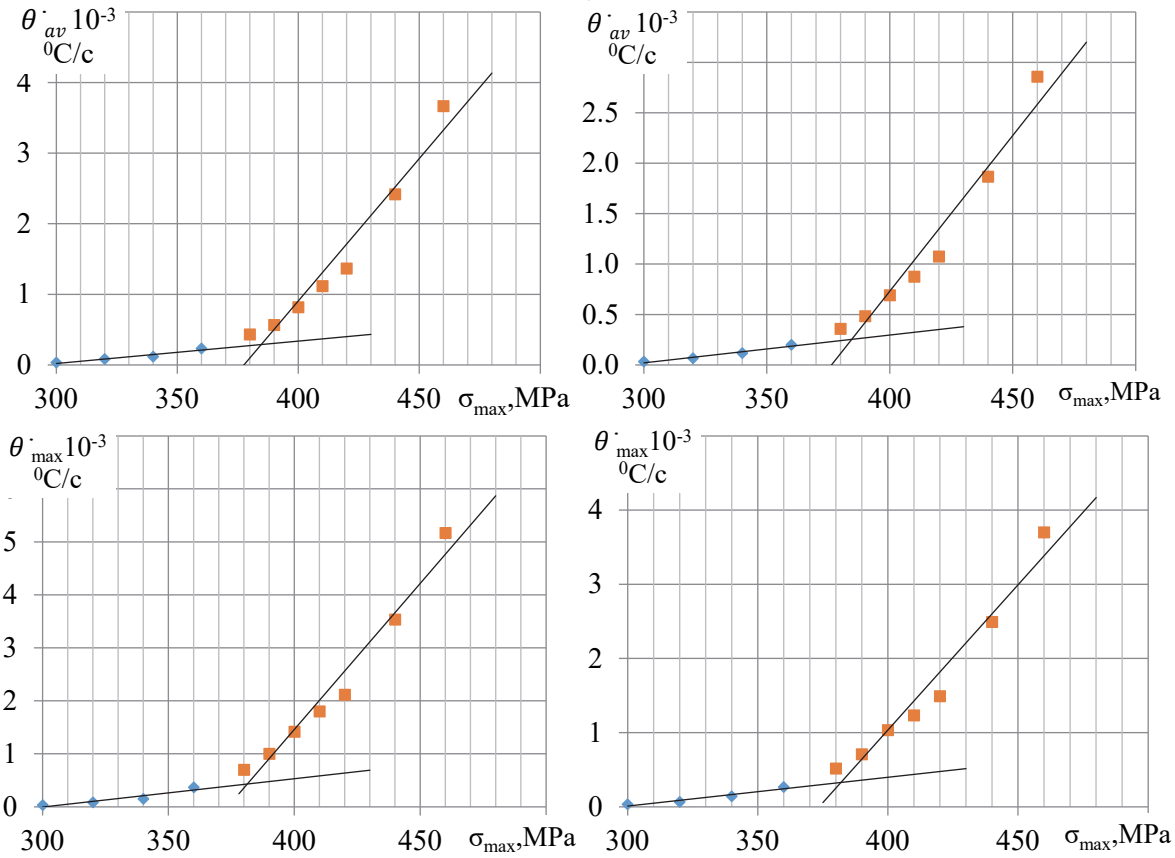

Figure 9: Determination of the fatigue limit using the derivative of the average (top left and top right) and maximum (bottom left and bottom right) temperatures at the beginning of each block for ΔN = 6000 and 12 000 cycles, respectively.

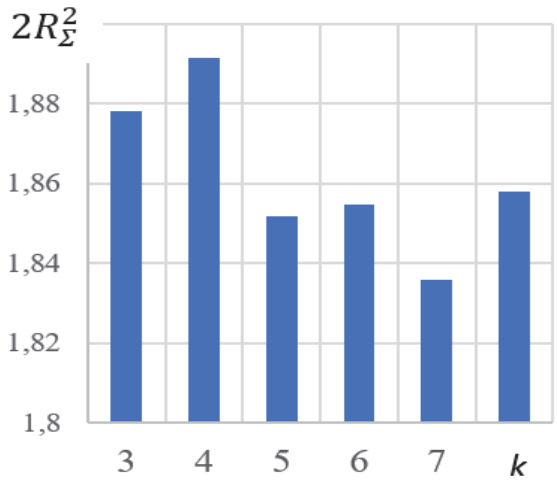

Figure 10: Example histogram of $R^2\Sigma$ for different separation points when processing temperature fields using the derivative of the average temperature at the block start.

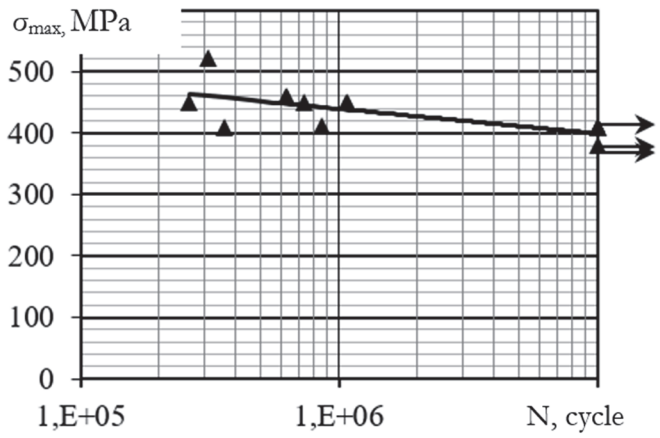

Figure 11: Results of fatigue tests of specimen batch by the traditional method.

The discrepancy between the fatigue limit values obtained by the standard method and the accelerated infrared thermography method is 4%. This discrepancy is insignificant against the background of the scattering of the experimental data obtained from the fatigue curve by the traditional method. Good agreement with the results of traditional fatigue tests can serve as a justification for the applicability of the Risitano method for determining the fatigue limit of nickel WAAM materials. In addition, the fatigue limit values obtained in this work by the Risitano method for WAAM alloy Inconel 625 are consistent with the data presented in the work of N. Martin et al. [8] for the same material Inconel 625 obtained by the hybridization of two laser-powder based additive processes. The fatigue limit values of 400-450 MPa presented by N. Martin et al. are close to those obtained in this work.

CONCLUSION

An accelerated method for evaluating the fatigue limit of nickel alloys manufactured by wire-arc additive technology has been developed within the infrared thermography framework. The method is based on the self-heating effect during cyclic loading.

The method development involved selecting specimen design, test equipment, number and parameters of loading blocks, self-heating indicators and data-processing procedures tailored to the material under investigation. When choosing specimen geometry and testing machine, it is advisable to ensure the possibility of cyclic loading frequencies more 100 Hz. For temperature recording, an infrared camera with high sensitivity and spatial resolution is recommended; the temperature range need not be wide—from room temperature to 100 °C.

Based on the conducted research, the following method parameters can be recommended for nickel alloys: at least 10 loading blocks; 6000–12 000 cycles per block; and a 10–20 MPa step increase in maximum stress from block to block.

It is shown that the rate of temperature rise at the specimen surface at the start of loading blocks can be used as a self-heating indicator. Using this parameter allows fewer fatigue damage cycles per block and thereby, if necessary, an increased number of blocks. It also reduces the overall experiment duration.

Experimental data on the fatigue limit of Inconel 625 specimens produced by WAAM were obtained. Validation was carried out by comparing the fatigue limit obtained by the accelerated method with results from conventional fatigue tests with an S–N curve. The difference between the two methods is only 4%, which lies within the scatter range of traditional fatigue tests.

For the additive nickel alloys investigated in this work, the infrared thermography-based accelerated fatigue-limit assessment enables a substantial reduction in both the number of specimens and test duration compared with traditional fatigue tests with an S–N curve. Consequently, the labour intensity and timeframe for selecting process parameters and refining additive manufacturing technologies can be significantly reduced.

ACKNOWLEDGEMENT

The research was financially supported by the Ministry of Science and Higher Education of the Russian Federation under state assignment “Development of scientific and technological foundations for the formation of material–structure systems with special properties based on hybrid additive technologies” – FSNM-2024-0003.

REFERENCES

[1] Panov, D., Permyakov, G., Naumov, S., Mirontsov, V., Kudryavtsev, E., Sun, L., Aksenov, A., Stepanov, N., Trushnikov, D., Salishchev, G. (2025). The Effect of Post-Deposition Heat Treatment on the Microstructure, Texture, and Mechanical Properties of Inconel 718 Produced by Hybrid Wire-Arc Additive Manufacturing with Inter-Pass Forging, 15, 78. DOI: https://doi.org/10.3390/met15010078

[2] Kindermann, R. M., Roy, M. J., Morana, R., Francis, J.A. (2022). Effects of microstructural heterogeneity and structural defects on the mechanical behaviour of wire + arc additively manufactured Inconel 718 components, Mater. Sci. Eng. A., 839, 142826.

[3] Hönnige J., Seow, C. E., Ganguluy, S., Xu, X., Cabeza, S., Coules, H., Williams, S., (2021). Study of residual stress and microstructural evolution in as-deposited and inter-pass rolled wire plus arc additively manufactured Inconel 718 alloy after ageing treatment, Mater. Sci. Eng. A., 801, 140368.
[4] Khomutinin, I.S., Varushkin, S.V., Stashkov, D.V., Trushnikov, D.N., Batrov, G.A. (2024). Study of the formation of single beads from Inconel 718 alloy by a distributed laser beam. Bulletin of PNIPU. Mechanical engineering, materials science. 26(3), pp. 66-73.
[5] Liu, H., Yu, H., Guo, C., Chen, X., Zhong, S., Zhou, L., Osman, A., Lu, J. (2024). Review on Fatigue of Additive Manufactured Metallic Alloys: Microstructure, Performance, Enhancement, and Assessment Methods, Adv. Mater., 36, 2306570. DOI: https://doi.org/10.1002/adma.202306570
[6] Cao, F., Zhang, T., Ryder, M. A., Lados, D. (2018). A Review of the Fatigue Properties of Additively Manufactured Ti-6Al-4V. The Journal of the Minerals, Metals & Materials Society. DOI: https://doi.org/10.1007/s11837-017-2728-5
[7] Concli, F., Gerosa, R., Panzeri, D., Fraccaroli, L. (2924). High and low cycle fatigue properties of additively manufactured Inconel 625, Progress in Additive Manufacturing, 9, pp. 1921–1940. DOI: https://doi.org/10.1007/s40964-023-00545-1
[8] Martin, N., Hor, A., Copin, E., Lours, P., Ratsifandrihana, L. (2023). Fatigue properties of as-built and heat-treated Inconel 625 obtained by the hybridization of two laser-powder based additive processes. International Journal of Fatigue, 172, 107650. DOI: https://doi.org/10.1016/j.ijfatigue.2023.107650.
[9] La Rosa, G., Risitano, A. (2000). Thermographic methodology for rapid determination of the fatigue limit of materials and mechanical components. Int. J. Fatigue, 22, pp. 65–73.
[10] Luong, M.P. (1998). Fatigue limit evaluation of metals using an infrared thermographic technique. Mech. Mater., 28, pp. 155–163.
[11] Fargione, G., Geraci, A., La Rosa, G., Risitano, A. (2002). Rapid determination of the fatigue curve by the thermographic method, International Journal of Fatigue. 24(1), pp. 11-19. DOI: https://doi.org/10.1016/S0142-1123(01)00107-4.
[12] Zaeimi, M., De Finis, R., Palumbo, D., Galietto, U. (2024). Fatigue limit estimation of metals based on the thermographic methods: A comprehensive review, Fatigue Fract Eng Mater Struct. 47, pp. 611–646. DOI: https://doi.org/10.1111/ffe.14206.
[13] Wei, W., He, L., Sun, Y., Yang, X. (2024). A. Review of Fatigue Limit Assessment Using the Thermography Based Method., Metals, 14, 640. DOI: https://doi.org/10.3390/met14060640
[14] Huang, J., Pastor, M.-L., Garnier, C., Gong, X.J. (2017). Rapid evaluation of fatigue limit on thermographic data analysis, International Journal of Fatigue, 104, pp. 293-301
[15] Zhao, Y., Lin, Z., Xia, Y., Chen, L., Gu, G., Pan, L. (2025). Fatigue-Limit Assessment via Infrared Thermography for a High-Strength Steel, Materials, 18, 279. DOI: https://doi.org/10.3390/ ma18020279
[16] Risitano, A., Risitano, G. (2010). Cumulative damage evaluation of steel using infrared thermography, Theoretical and Applied Fracture Mechanics, 54(2), pp. 82-90. DOI: https://doi.org/10.1016/j.tafmec.2010.10.002;
[17] Yang, W., Guo, X., Guo, Q., Fan, J. (2019). Rapid evaluation for high-cycle fatigue reliability of metallic materials through quantitative thermography methodology, International Journal of Fatigue, 124, pp. 461-472. DOI: https://doi.org/10.1016/j.ijfatigue.2019.03.024
[18] Ricotta, M., Meneghetti, G., Atzori, B., Risitano, G., Risitano, A. (2019). Comparison of experimental thermal methods for the fatigue limit evaluation of a stainless steel, Metals 9, 677; DOI: https://doi.org/10.3390/met9060677.
[19] Plekhov, O.A., Naimark, O.B., Valievb, R. Z., Semenov, I. P., Saintierc, N., Palin-Luc, T. (2008). Experimental Investigationsof Anomalous Energy Absorptionin Nanocrystalline Titanium under Cyclic Loading Conditions, Technical physics letters. 34(7), pp. 557-560
[20] Santoro, L., Sesana, R., Diller, J., Radlbeck, C., Mensinger, M. (2024). Dissipative and thermal aspects in cyclic loading of additive manufactured AISI 316L, Engineering Failure Analysis 163, 108446.
[21] Zhang, H., Li, C., Song, W, He, N., Wang, F., Zhang, Y. (2023). Fatigue life evaluation and cellular substructure role of laser powder bed fused 304L steel based on dissipative deformation mechanisms, Additive Manufacturing 64, 103430.
[22] Douellou, C., Balandraud, X., Duc, E., Verquin, B., Lefebvre, F., Sar, F. (2020). Rapid characterization of the fatigue limit of additive-manufactured maraging steels using infrared measurements, Additive Manufacturing. 35, 101310. DOI: https://doi.org10.1016// j.addma.2020.101310
[23] Zhao, A., Xie, J., Zhao, Y., Liu, C., Zhu, J., Qian, G., Wang, S., Hong, Y. (2022). Fatigue limit evaluation via infrared thermography for a high strength steel with two strength levels, Engineering Fracture Mechanics 268, 108460.
[24] Solomonov, D.G., Nikhamkin, M.Sh. (2025). Accelerated assessment of the fatigue limit of polymer composite materials by infrared thermography. Factory laboratory. Diagnostics of materials. 91(2), pp. 76–84. DOI: https://doi.org/10.26896/1028-6861-2025-91-2-76-84.